Electrical characteristics of rock samples from the La Ronge Domain of the Trans-Hudson Orogen, northern Saskatchewan

T.J. Katsube, A.G. Jones[1], N. Scromeda, and P. Schwann[2]
Mineral Resources Division, Ottawa

Katsube, T.J., Jones, A.G., Scromeda, N., and Schwann, P., 1996: Electrical characteristics of rock samples from the La Ronge Domain of the Trans-Hudson Orogen, northern Saskatchewan; in Current Research 1996-E; Geological Survey of Canada, p. 159-169.

Abstract: Electrical resistivities of rock samples (gneiss, greywacke and argillite), obtained from the western part of the La Ronge Domain, were studied to determine the source of elevated electrical conductivities observed deep in the subsurface of the region.

Analyses show that the resistivities of these rocks cover a wide range of values (0.3-2x10^4 Ω·m). While the larger values are typical for these types of rocks, the smaller ones are likely due to layers (thicknesses of about 1-5 mm) of sulphide concentrations. These layers are also a source of significant electrical resistivity anisotropy. These rocks are folded, with sulphide layers accumulated near the hinge of the fold forming a source of high electrical conductivity along its axis. Generally, the resistivities are 3-8 Ω·m in the direction of the fold axis, and 2000-20 000 Ω·m for samples from the host gneissic rock, which gives a bulk anisotropy of 200:1 to 7000:1 for the metasedimentary unit.

Résumé : La résistivité électrique d'échantillons de roches (gneiss, grauwacke et argilite) provenant de la partie ouest du Domaine de La Ronge a été mesurée pour déterminer la source des valeurs élevées de conductivité électrique observées dans les lithologies profondes de la région.

Les analyses indiquent que les valeurs de résistivité de ces lithologies couvrent un large intervalle (de 0,3 x 10^4 Ω·m à 2,0 x 10^4 Ω·m). Les valeurs les plus élevées sont caractéristiques des types de roches susmentionnées; quant aux valeurs faibles, elles sont probablement attribuables à des couches sulfurées (épaisseurs variant entre environ 1 et 5 millimètres). Ces couches sont en outre la source d'une anisotropie significative de la résistivité électrique. Les roches sont plissées et les couches sulfurées sont concentrées près de la charnière du pli, formant une source de conductivité électrique élevée le long de son axe. Généralement, les valeurs de résistivité atteignent 3-8 Ω·m dans la direction de l'axe du pli et 2 000-20 000 Ω·m dans les échantillons provenant de la roche gneissique hôte, ce qui donne une anisotropie apparente de 200:1 à 7 000:1 dans le cas de l'unité métasédimentaire.

[1] Continental Geoscience Division, Ottawa
[2] Saskatchewan Northern Affairs, Box 5000, La Ronge, Saskatchewan S0J 1L0

INTRODUCTION

Brief history of the discovery and early investigations of the NACP anomaly

The North American Central Plains (NACP) anomaly in electrical conductivity was discovered on the edge of an array of magnetometers by Gough and his colleagues in 1967 (Reitzel et al., 1970), and then located in the Black Hills region by a second array study in 1969 (Camfield et al., 1970; Porath et al., 1970, 1971; Gough and Camfield, 1972; Camfield and Gough, 1975). A subsequent magnetometer array in the Dakotas and Saskatchewan in 1972 traced the anomaly through those states and province (Alabi et al., 1975), and two later profiles of magnetometers tracked it through northern Saskatchewan and northern Manitoba (Handa and Camfield, 1984; Gupta et al., 1985; respectively). This curvi-linear feature, which affects natural electromagnetic fields from 10 s periodicity to periods of greater than one cycle per day, is estimated to be of at least 2000 km in length, and possibly connects to conductivity anomalies in Scandinavia (Jones, 1993). As such, it is the largest coherent crustal anomaly of enhanced electrical conductivity yet discovered.

In a bold and intuitive paper, Camfield and Gough (1977) suggested that the NACP was a geophysical expression of a Proterozoic plate boundary buried beneath the Phanerozoic cover of the mid-North American continent. Geological and geochronological investigations, using samples from basement-reaching boreholes (Peterman, 1981; Klasner and King, 1986), and interpretations of potential field maps (Green et al., 1979, 1985; Dutch, 1983; Klasner and King, 1986; Thomas et al., 1987) confirmed this subsurface extrapolation of structures exposed in northern Saskatchewan and Manitoba identified in the mid-1970s as an orogenic zone, termed the Trans-Hudson Orogen (THO) by Hoffman (1981), with a proposed Proterozoic plate boundary in southern Wyoming by Hills et al. (1975).

PanCanadian Oil Co. Ltd. was interested in basement control of sedimentary structures, and contracted a magnetotelluric (MT) survey over the NACP anomaly just north of the U.S./Canadian border in southern Saskatchewan in 1984. Due to the large spatial separation of Alabi et al.'s (1975) magnetometer sites (typically 75 km or greater), the actual position of the anomaly was mislocated, and a second survey farther east was undertaken in 1985 (Jones and Savage, 1986). This showed definitively that the NACP anomaly was located some 75 km east of the position identified by the array study. This view was contended by Maidens and Paulson (1988), but the comment on their paper and interpretation by Jones (1988), who pointed out their errors and stated that the NACP anomaly does indeed lie as detailed by Jones and Savage (1986), went unchallenged. Modeling of the PanCanadian MT data illustrated that the anomalies in electrical conductivity causing the anomaly were in the crust, and were arcuate in form with the centre of the arch being at about 103.25°W in southern Saskatchewan (Jones and Craven, 1990). A second major enhancement was also identified and named the TOBE anomaly because of the along-strike spatial association of aeromagnetic maps with the postulated subsurface extrapolation of the Thompson Belt (Jones and Craven, 1990; Rankin and Pascal, 1990). Two further MT profiles across the anomaly in central Saskatchewan illustrated that it is not a continuous feature, as implied by the magnetometer array work, and that it is displaced some 75 km to the west at around a latitude of 52°N (Jones and Craven, 1990).

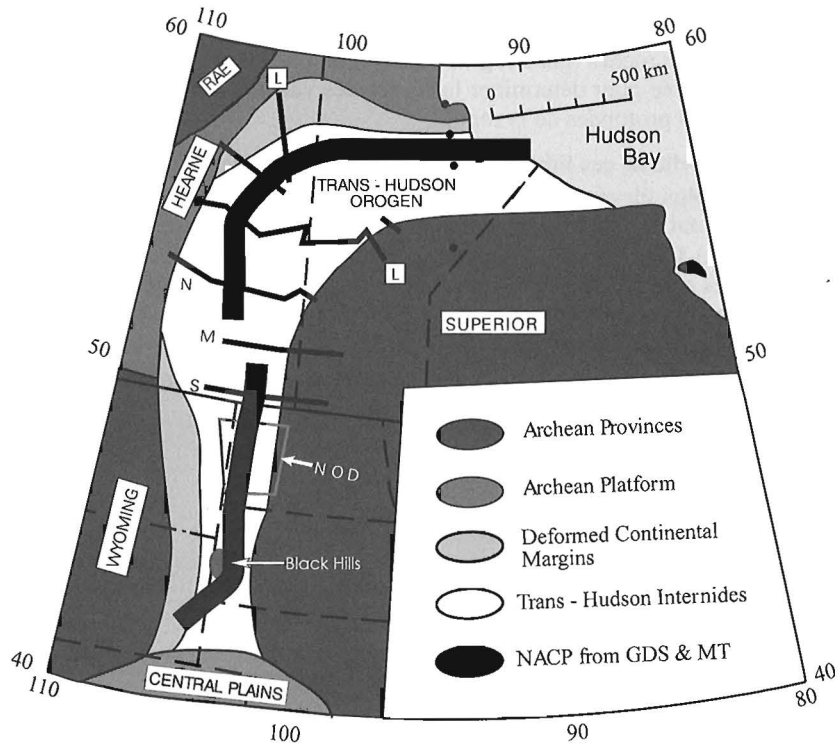

Figure 1.

Cartoon map of basement elements showing the Trans-Hudson Orogen (THO) and the trace of the North American Central Plains (NACP). S, M, N: South, Mid and North Saskatchewan MT profiles of Jones and Craven (1990); NOD: North Dakota MT studies by the University of Washington and the Geological Survey of Canada (unpubl.); L: Lithoprobe MT profiles.

Seismic reflection profiling in northern North Dakota imaged an arcuate non-reflecting deep crustal body with reflecting packages that lay on top of it. These reflecting packages correlated spatially with the locations of the zones of enhanced conductivity imaged by Jones and Craven (1990) just to the north (Nelson et al., 1993).

Figure 1 illustrates the trace of the NACP anomaly from all the above studies together with the generalized basement map of central North America. Note that the NACP lies virtually wholly within the Trans-Hudson Orogen, and is, for the most part, on its western or northern boundary.

Lithoprobe MT studies

Under the auspices of Lithoprobe (Clowes et al., 1993), magnetotelluric experiments have been undertaken on two campaigns. One in 1992 of 110 sites, and the other in 1994 of 30 sites. The 1992 experiment was along a single profile from one bounding craton (Superior to the east) to the other (Rae/Hearne to the west). The lines in Saskatchewan and the lithotectonic elements are shown in Figure 2. The MT data from the western part of the 1992 transect have been analyzed and modelled, and show that the NACP anomaly is associated with the western part of the La Ronge Domain, and that it dips beneath the Rottenstone Domain and the Wathaman Batholith, and ends at the Needle Falls Shear Zone (Jones et al., 1993). The model is illustrated in Figure 3, with the major seismic interfaces, determined from the reflection section, in bold lines.

Cause of enhanced conductivity

The actual cause of the enhanced conductivity in the NACP anomaly has been the subject of speculation since its discovery. Camfield and Gough (Camfield et al., 1970; Gough and Camfield, 1972; Camfield and Gough, 1977), considering the spatial correlation of the southern end of the NACP with graphitic schistose rocks in a belt mapped by Lidiak (1971), suggested that the enhanced conductivity is due to graphite sheets in highly metamorphosed and folded basement rocks. Green et al. (1985) suggested that it is due to partial serpentinization of oceanic mafic and ultramafic rocks at the ridge

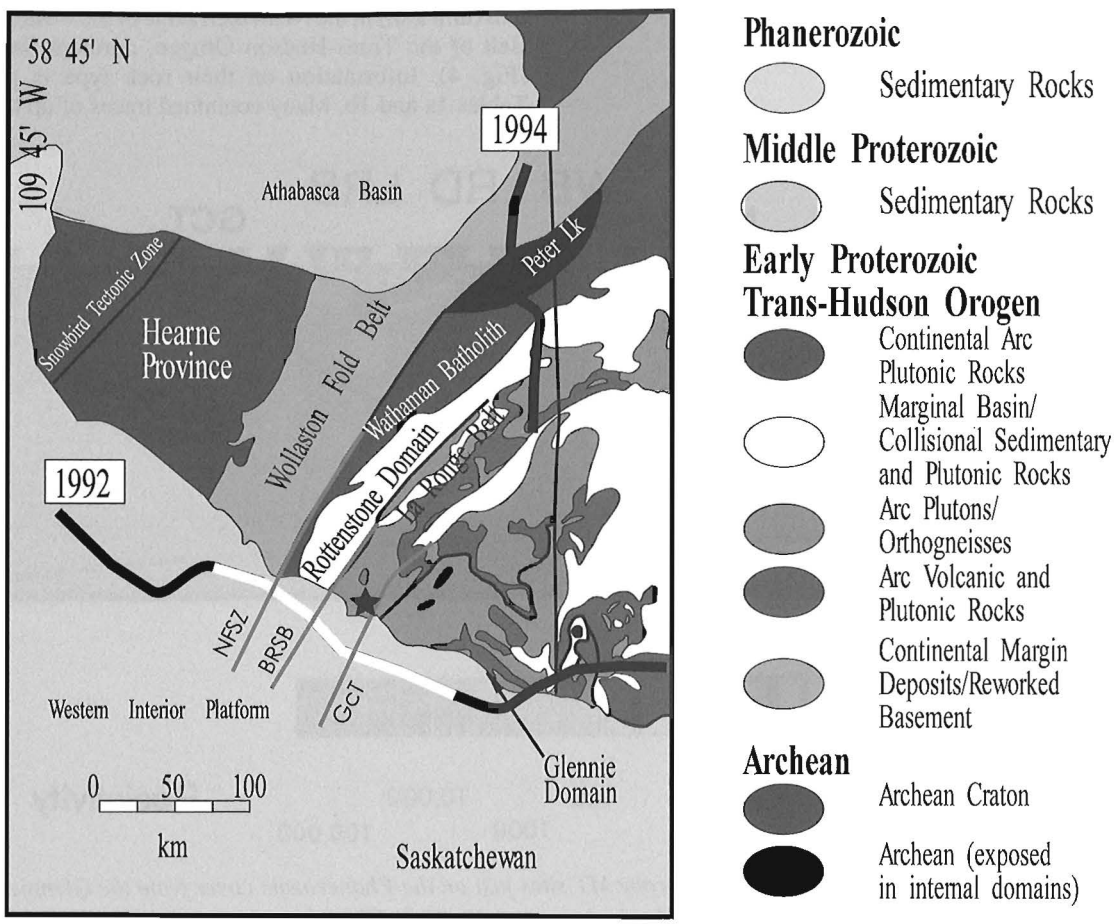

Figure 2. *Lithotectonic elements of the Trans-Hudson Orogran in Saskatchewan. The 1992 and 1994 MT profiles shown as solid lines, with that part of the 1992 profile modelled in Figure 3 in white. NFSZ: Needle Falls Shear Zone; BRSB: Birch Rapids Straight Belt; GcT: Guncoat Thrust. The star indicates the location of the rock samples in Figure 4.*

crest of ancient former oceanic crust, and Handa and Camfield (1984) proposed that it is due to trapped saline water in fractured rocks.

The conclusive spatial correlation of the NACP anomaly with the western La Ronge Domain by the 1992 Lithoprobe MT studies (Jones et al., 1993) gave an opportunity to identify the actual cause of enhanced conductivity. The anomaly is bounded by two high strain packages; the Guncoat Thrust and the Birch Rapids Straight Belt (Fig. 2). Within these packages are the only significant occurrences of graphite in the region (J.F. Lewry, pers. comm., 1993), but the data show that these bounding zones are not conductive compared to the units in between. The rocks within the western La Ronge Domain are mainly granodioritic-granitic gneisses interleaved with minor, discontinuous pelitic to psammitic sedimentary and plutonic rocks (Lewry and Slimmon, 1985), and associated mineralization, with economic deposits of gold, nickel, and copper in disjointed vein and disseminated sulphides, in the metasedimentary sequences. Conductors mapped by airborne electromagnetic surveys (compiled by Standing, 1973) are long, linear features that correlate spatially with surface exposures of the biotitic metasedimentary rocks. These observations led Jones et al. (1993) to associate the NACP anomaly with sulphides in the western La Ronge Belt.

Rock property studies

In order to determine conclusively the source of elevated electrical conductivities observed deep in the subsurface of the region, electrical resistivities of rock samples (gneiss, greywacke, and argillite) obtained from unit Lsn (L=La Ronge; sn=sedimentary), a biotitic metasedimentary unit in the western part of the La Ronge Domain of the Trans-Hudson Orogen, were measured. The electrical resistivity measurements were conducted in all three directions of the samples to ascertain the extent of electrical anisotropy in the rocks, and whether it might be related to the source of these subsurface anomalies. Hand-sample sized specimens were collected from seven locations deemed representative of the unit in the Nemeiben Zone of the western La Ronge Domain (Fig. 4).

METHOD OF INVESTIGATION

Samples and sample preparation

Seven rock samples (gneiss, greywacke, and argillite), each consisting of several sub-samples, and each weighing about 1-10 kg, were collected from the biotitic metasedimentary unit (unit Lsn) in the Nemeiben Zone of the western La Ronge Belt of the Trans-Hudson Orogen, northern Saskatchewan (Fig. 4). Information on their rock type is provided in Tables 1a and 1b. Many contained traces of up to 5 per cent

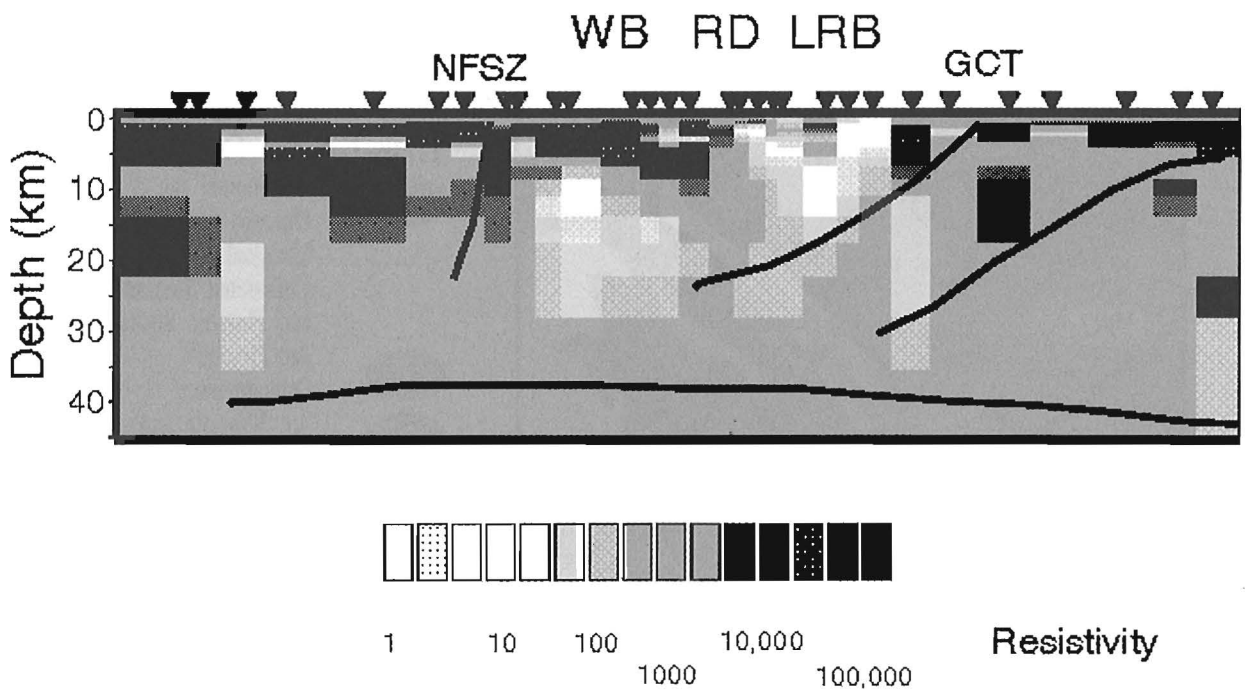

Figure 3. *Resistivity model from the Lithoprobe MT sites just on the Phanerozoic cover from the Glennie Domain to the Rae/Hearne craton (Fig. 2). Vertical exaggeration 1:1. White denotes resistivities <50 Ω·m, whereas black denotes resistivities >1000 Ω·m. The solid lines are from the seismic reflection section showing (a) the presumed projection of the Needle Falls Shear Zone (NFSZ), (b) the Guncoat Thrust (GCT), and (c) the top surface of the Archean microblock of unknown affinity, named the Sask craton. WB=Wathaman Batholith; RD=Rottenstone Domain; LRB=La Ronge Belt.*

Table 1a. Sample locations.

Sample	Location Description
LP94-001	On the Nemeiben Lake road
LP94-002	as LP94-001
LP94-003	as LP94-001
LP94-004	On the north side of English Bay
LP94-005	West side of Contact Lake
LP94-006	East side of MacKay Lake
LP94-007	On the Stanley Mission road close to Sulphide Lake

Table 1b. Sample information (rock type and strike/dip).

Sample	Rock Type	Strike/Dip
LP94-001	Quartz-feldspar-biotite gneiss	160/75SW
LP94-002	Quartz-feldspar-biotite gneiss	168/78SW
LP94-003	Quartz-feldspar-biotite gneiss	168/vert
LP94-004	Quartz-feldspar-muscovite gneiss with muscovite porphyroblasts	20/65SE
LP94-005	Biotite porphyroblastic greywaycke	-
LP94-006	Greywaycke	76/82S
LP94-007	Carbonaceous sulphidic argillite	72/70S

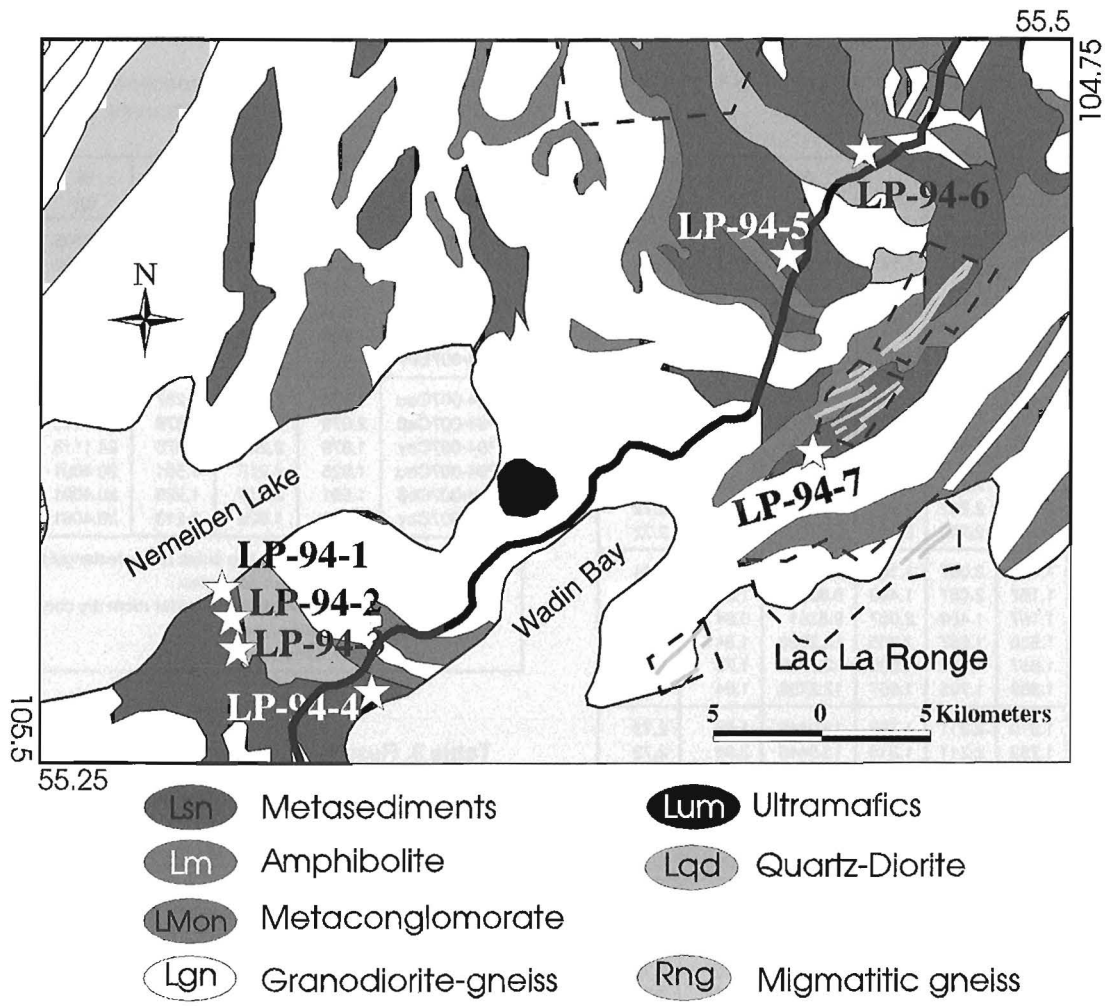

Figure 4. *Rock sampling locations. Lsn: Biotitic metasedimentary unit in the La Ronge Domain; Lm: La Ronge amphibolite, hornblende gneiss and schist; Lum: La Ronge ultramafic rocks; Lqd: La Ronge quartz diorite-granodiorite-quartz monzonite-granite; Lgn: Granodiorite-granite complex; Rng: Birch Rapids Strait Belt – Migmatitic gneiss of the Rottenstone Domain. The dashed boxes show the regions where airborne EM observations were flown, and the solid lines indicate the locations of conductors mapped (Standing, 1973).*

(estimate) sulphides. These 7 samples are represented by numbers LP94-001 to LP94-007. One to three sub-samples were selected as representative of each sample. In the case of sample LP94-007, the three sub-samples are coded with the letters A, B and C following the seven digit sample numbers. A second series of one to three sub-samples, represented by the letters a, b and c following the 7-8 digit sample or sub-sample numbers, were cut out from each sample or sub-sample. This amounts to a total of 15 sub-samples. One to two specimens were cut out of each sub-sample, one for bulk density (δ) and electrical resistivity (ρ_r) and one for effective porosity (ϕ_E) determinations. Those prepared for bulk density and electrical resistivity measurements were cut into rectangular shapes so that the latter could be measured in all three directions, identified by α, ß and γ. Those prepared for effective porosity measurements were either rectangular or irregular in shape. The δ and ρ_r measurements were performed on all 15 sub-samples, and ϕ_E on only 12 of these sub-samples containing no visible sulphides. The geometric characteristics of the specimens used for ρ_r and δ measurements are listed in Tables 2a and 2b. The dimensions are in the range of 1.3-2.2 cm for the rectangular shaped specimens.

Bulk density and effective porosity measurements

The caliper method (API, 1960) has been used to determine the bulk density, δ, of the samples, by measuring the dimensions and weight of the rectangular specimens. This measurement constitutes part of the porosity determining procedure. Effective porosity, ϕ_E, in principle represents the pore volume of all interconnected pores. In this study, it is determined from the difference in weight between the oven-dried and water-saturated rock specimen.

Table 2a. Dimensions of specimens cut out from the samples for electrical measurements.

Sample	a_1 (cm)	a_2 (cm)	ℓ (cm)	W (g)	K_G (10^{-2}m)	δ (g/mL)
LP94-001α	1.741	2.219	1.405	14.5982	2.75	2.69
LP94-001β	1.405	2.219	1.741	14.5982	1.79	2.69
LP94-001γ	1.405	1.741	2.219	14.5982	1.10	2.69
LP94-002aα	1.493	1.744	1.386	9.7645	1.88	2.71
LP94-002aβ	1.386	1.744	1.493	9.7645	1.62	2.71
LP94-002aγ	1.386	1.493	1.744	9.7645	1.19	2.71
LP94-002bα	1.487	1.571	1.617	10.2456	1.45	2.71
LP94-002bβ	1.571	1.617	1.487	10.2456	1.71	2.71
LP94-002bγ	1.487	1.617	1.571	10.2456	1.53	2.71
LP94-003α	2.205	2.242	2.210	29.7555	2.24	2.72
LP94-003β	2.210	2.242	2.205	29.7555	2.25	2.72
LP94-003γ	2.205	2.210	2.242	29.7555	2.17	2.72
LP94-004aα	1.489	2.067	1.167	9.8381	2.64	2.74
LP94-004aβ	1.167	2.067	1.489	9.8381	1.62	2.74
LP94-004aγ	1.167	1.489	2.067	9.8381	0.84	2.74
LP94-004bα	1.589	1.657	1.705	12.2792	1.54	2.74
LP94-004bβ	1.657	1.705	1.589	12.2792	1.78	2.74
LP94-004bγ	1.589	1.705	1.657	12.2792	1.64	2.74
LP94-005α	1.319	2.211	1.753	13.9446	1.66	2.73
LP94-005β	1.753	2.211	1.319	13.9446	2.94	2.73
LP94-005γ	1.319	1.753	2.211	13.9446	1.05	2.73
LP94-006α	1.612	2.251	1.522	15.6995	2.38	2.84
LP94-006β	1.522	2.251	1.612	15.6995	2.13	2.84
LP94-006γ	1.522	1.612	2.251	15.6995	1.09	2.84
LP94-007Aaα	1.644	2.233	1.583	16.0573	2.32	2.76
LP94-007Aaβ	1.583	2.233	1.644	16.0573	2.15	2.76
LP94-007Aaγ	1.583	1.644	2.233	16.0573	1.17	2.76
LP94-007Abα	1.516	2.150	1.808	16.2846	1.80	2.76
LP94-007Abβ	1.808	2.150	1.516	16.2846	2.56	2.76
LP94-007Abγ	1.516	1.808	2.150	16.2846	1.28	2.76
LP94-007Acα	1.619	2.087	1.572	16.6943	2.15	3.14
LP94-007Acβ	1.572	2.087	1.619	16.6943	2.03	3.14
LP94-007Acγ	1.572	1.619	2.087	16.6943	1.22	3.14

a_1, a_2: Length of the two sides of the rectangular specimen.
ℓ: Thickness of specimen.
W: Weight of specimen under room dry conditions.
K_G: Geometric factor.
δ: Bulk density

Table 2b. Dimensions of specimens cut out from the samples for electrical measurements.

Sample	a_1 (cm)	a_2 (cm)	ℓ (cm)	W (g)	K_G (10^{-2}m)	δ (g/mL)
LP94-007Baα	1.785	2.159	1.619	17.0605	2.38	2.73
LP94-007Baβ	1.619	2.159	1.785	17.0605	1.96	2.73
LP94-007Bay	1.619	1.785	2.159	17.0605	1.34	2.73
LP94-007Bbα	1.824	2.379	1.926	25.1178	2.25	3.01
LP94-007Bbβ	1.926	2.379	1.824	25.1178	2.51	3.01
LP94-007Bbγ	1.824	1.926	2.379	25.1178	1.48	3.01
LP94-007Caα	1.878	2.079	2.267	24.1118	1.72	2.72
LP94-007Caβ	2.079	2.267	1.878	24.1118	2.51	2.72
LP94-007Cay	1.878	2.267	2.079	24.1118	2.05	2.72
LP94-007Cbα	1.925	2.213	1.591	20.4091	2.68	3.01
LP94-007Cbβ	1.591	2.213	1.925	20.4091	1.83	3.01
LP94-007Cbγ	1.591	1.925	2.213	20.4091	1.38	3.01

a_1, a_2: Length of the two sides of the rectangular specimen.
ℓ: Thickness of specimen.
W: Weight of specimen under room dry conditions.
K_G: Geometric factor.
δ: Bulk density

Table 3. Results of the effective porosity measurements.

Sample	δ (g/mL)	W_W (g)	W_D (g)	S_{ir} (%)	ϕ_E (%)
LP94-001	2.69	7.0147	6.9737	22.4	1.58
LP94-002	2.71	10.0792	9.9948	19.7	2.29
LP94-003	2.72	9.2004	9.1618	17.6	1.15
LP94-004a	2.74	6.5180	6.4977	24.1	0.86
LP94-004b	2.74	7.5839	7.5644	25.1	0.71
LP94-005	2.73	5.6994	5.6557	11.2	2.11
LP94-006	2.84	10.3938	10.3662	27.9	0.76
LP94-007Aa	2.76	6.3161	6.1386	21.7	7.98
LP94-007Ab	2.76	10.2831	10.1036	32.6	4.90
LP94-007Ac	3.14	7.4826	7.4094	51.5	3.10
LP94-007B	3.01	4.7395	4.6970	38.4	2.72
LP94-007C	3.01	7.9944	7.9390	40.1	2.10

W_w = wet weight
δ = bulk density (Equation 2)
S_{ir}= irreducible water saturation
ϕ_E = effective porosity
W_D = dry weight

The API Recommended Practice for Core-Analysis Procedures (API, 1960) has generally been followed in these measurements. The procedures routinely used in our measurements are described in the literature (Katsube and Scromeda, 1991; Katsube et al., 1992a; Scromeda and Katsube, 1994).

Bulk electrical resistivity measurements

The bulk electrical resistivity, ρ_r, is determined from the complex electrical resistivity (ρ^*) measurements made by methods described in recent publications (e.g. Katsube, et al., 1991; Katsube and Salisbury, 1991; Katsube and Scromeda, 1994). ρ^* is measured over a frequency range of 1-10^6 Hz, with ρ_r representing a bulk electrical resistivity at frequencies of about 10^2-10^3 Hz. It is a function of the pore structure and pore fluid resistivity, and is understood to exclude any other effects, such as pore surface, dielectric or any other polarizations (Katsube, 1975; Katsube and Walsh, 1987), including electrode polarization.

Table 4a. Results of electrical resistivity measurements.

Sample	Mes. #1	ρ_r, (10^3 Ωm) Mes. #2	Mean
LP94-001α	5.48	9.64	7.56
LP94-001β	2.03	3.57	2.80
LP94-001γ	1.85	2.97	2.41
LP94-002aα	14.37	14.27	14.32*
LP94-002aβ	11.49	12.29	11.89*
LP94-002aγ	9.51	8.45	8.98*
LP94-002bα	12.41	9.47	10.94*
LP94-002bβ	14.15	12.28	13.22*
LP94-002bγ	12.82	11.72	12.27*
LP94-003α	20.48	21.26	20.87*
LP94-003β	16.40	19.51	17.96
LP94-003γ	14.27	18.22	16.25
LP94-004aα	10.50	10.86	10.68
LP94-004aβ	5.88	6.91	6.40
LP94-004aγ	5.62	6.02	5.82
LP94-004bα	9.41	8.78	9.10
LP94-004bβ	12.71	12.56	12.64*
LP94-004bγ	10.31	10.68	10.50
LP94-005α	13.67	12.83	13.25
LP94-005β	15.06	14.55	14.81
LP94-005γ	8.27	8.59	8.43*
LP94-006α	3.56	3.95	3.76
LP94-006β	4.59	5.21	4.90
LP94-006γ	7.28	9.16	8.22*
LP94-007Aaα	0.020	0.017	0.019
LP94-007Aaβ	0.29	0.28	0.29
LP94-007Aaγ	0.033	0.032	0.033
LP94-007Abα	0.023	0.022	0.023
LP94-007Abβ	0.39	0.25	0.32
LP94-007Abγ	0.050	0.053	0.052
LP94-007Acα	0.0011	0.0009	0.0010
LP94-007Acβ	0.0006	0.0004	0.0005
LP94-007Acγ	0.0003	0.0002	0.0003

ρ_r= Bulk Electrical Resistivity.
Mes. (#1)= Measurement after 24 hours of saturation.
Mes. (#2)= Measurement after 48 hours of saturation.
*= Values determined from slightly distorted complex resistivity plots (Katsube et al., 1992).

EXPERIMENTAL RESULTS

The results of the bulk density (δ) determinations are listed in Tables 2a and 2b. They are in the range of 2.69-3.14 g/mL. The smaller values resemble those of a granitic gneiss (Daly et al., 1966), and the larger ones resemble those of a more basic rock. The results of the effective porosity (ϕ_E) measurements are listed in Table 3, displaying values in the range of 0.76-8.0%. The smaller values are typical of crystalline rocks (Katsube and Mareschal, 1993; Katsube and Scromeda, 1995) and the larger ones resemble those of a relatively competent sedimentary rock (Daly et al., 1966). In general, these porosities are relatively high for a crystalline rock.

The results of the electrical resistivity (ρ_r) measurements are listed in Tables 4a and 4b. Determinations have been made at 24 and 48 hours after water saturation, to ensure that they represent ρ_r values stable with time. Some examples of the complex resistivity plots used to determine the low values of ρ_r are shown in Figure 5. Details of this determination procedure are described elsewhere (e.g. Katsube and Scromeda, 1994). The ρ_r values are in the range of 0.3-2x10^4 Ω·m for these samples, the lower values in the range of rocks containing relatively large amounts of sulphides (Keller, 1982), and the higher values being typical of crystalline rocks (Katsube and Hume, 1987, 1989; Katsube and Mareschal, 1993). Some

Table 4b. Results of electrical resistivity measurements.

Sample	Mes. #1	ρ_r, (10^3 Ωm) Mes. #2	Mean
LP94-007Baα	0.40	0.25	0.33
LP94-007Baβ	1.35	0.60	0.98
LP94-007Baγ	5.74	1.94	3.84
LP94-007Bbα	0.049	0.046	0.048
LP94-007Bbβ	0.14	0.12	0.13
LP94-007Bbγ	0.0079	0.0077	0.0078
LP94-007Caα	0.089	0.076	0.083
LP94-007Caβ	0.89	0.68	0.79
LP94-007Caγ	0.53	0.46	0.50
LP94-007Cbα	0.015	0.014	0.015
LP94-007Cbβ	0.057	0.051	0.054
LP94-007Cbγ	0.0029	0.0032	0.0031

ρ_r= Bulk Electrical Resistivity.
Mes. (#1)= Measurement after 24 hours of saturation.
Mes. (#2)= Measurement after 48 hours of saturation.

complex resistivity plots showed slightly distorted arcs (Fig. 4a and 5a in Katsube et al., 1992b), implying that the ρ_r values obtained using these plots (denoted by an * in Table 4a) are likely to be slightly smaller than the true values.

DISCUSSION

The bulk densities observed (δ = 2.69-3.14 g/mL, Tables 2a and 2b) are not an unexpected range of values for these types of rocks. While the smaller effective porosity (ϕ_E=0.76-8.0%) values are typical of these types of crystalline rocks (Katsube and Mareschal, 1993; Katsube and Scromeda, 1995), the larger ones are not. Particularly, those displaying values above 3.0% (e.g. ϕ_E=4.9-8.0% for samples LP94-007Ab, LP94-007Aa) are unexpected for these rocks. This is probably a result of weathering, particularly of some of the sulphides, that has taken place because of these samples having been at or near the surface.

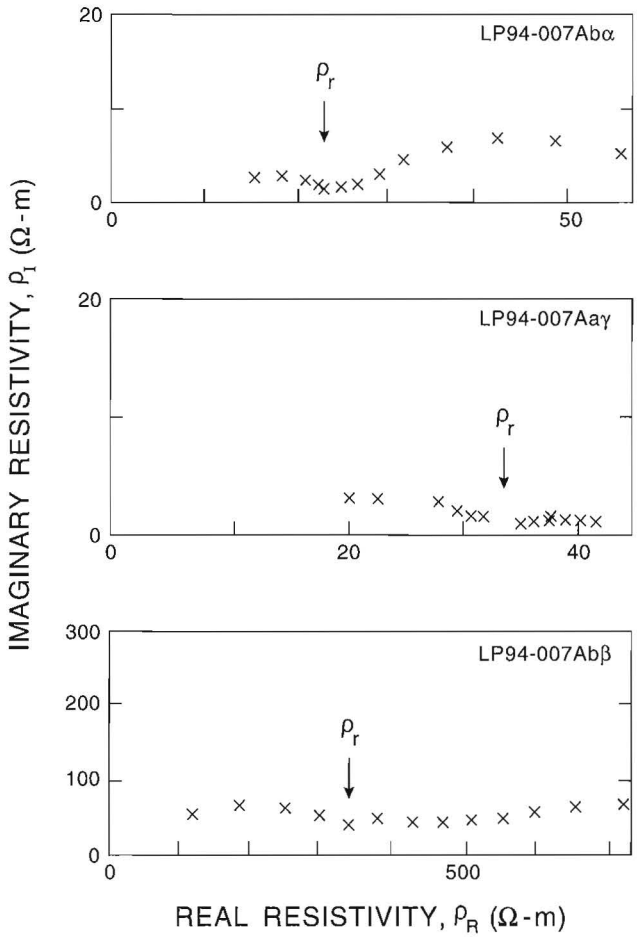

Figure 5. *Typical examples of complex resistivity plots used to determine low bulk electrical resistivity (ρ_r) values. These are examples for samples/specimens PL94-007Abα, PL94-007Aaγ, and PL94-007Abβ. Because of the low resistivities, strong electrode polarization effects (right-most arcs) are seen, but outside the range of influence on ρ_r. The relationship between ρ_I and ρ_R is described in the literature (e.g. Katsube and Walsh, 1987; Katsube et al., 1991, 1992b).*

The bulk electrical resistivities (ρ_r) of these rocks cover a wide range of values (ρ_r=0.3-2x10^4 Ω·m). While the larger values are typical for these types of rocks (Katsube and Mareschal, 1993; Katsube and Hume, 1987, 1989), the smaller values reflect effects of strong electrically conductive paths existing in some or some parts of these rocks. These are due to the visible layers, thicknesses of about 1-5 mm, which contain varied degrees of sulphide concentrations. These layers are a cause of significant electrical resistivity anisotropy, up to about 10:1 to 18:1, as seen in Tables 4a and 4b for samples/specimens LP94-007Ab, LP94-007Ba, LP94-007Bb, and LP94-007Cb.

The low ρ_r values (0.3-1.0 Ω·m) and large anisotropies of these rocks have significant implications on their bulk electrical characteristics. The slice of rock displayed in Figure 6 describes the distribution of layers of sulphide concentrations in sub-samples LP94-007B and LP94-007C. They both are parallel slices cut from sample LP94-007, and represent a cross-section of a folded rock with layers containing sulphides tending to concentrate towards the hinge of the fold. While the sulphide concentrations are not continuous along the folded bedding, they are continuous along the axis of the folding. Three discontinuous layers of sulphide concentrations are seen in this cross-section (Fig. 6), a highly concentrated thick layer (upper left), a highly concentrated thin layer (upper right), and a thick layer (lower section) with a low concentration of sulphides. A second series of three sub-samples (LP94-007Cb, LP94-007Bb, LP94-007Ba) representing these three layers, with very different sulphide concentration characteristics, were cut out of these two slices of rock.

The two second series of sub-samples (LP94-007Cb, LP94-007Bb), representing the highly concentrated layers, indicate resistivities of 3-8 Ω.m in the direction of the axis, and 15-130 Ω·m in the other two directions. If the resistivity values of the sections of the rock barren of sulphides (2000-20 000 Ω·m, Table 4a) are taken into consideration, the electrical model shown in Figure 7 can be constructed. This model represents the rock with folded layers containing highly concentrated sulphides accumulated near the head of the fold. These layers are discontinuous along the folded bedding, but continuous along the axis of the fold. When all the observed resistivity values are taken into consideration, this model suggests resistivities of 3-8 Ω·m in the direction of the axis, and 2000-20 000 Ω·m in the other two directions, an anisotropy of 200:1 to 7000:1. This model suggests an electrical anisotropy that has hitherto not been reported for laboratory studies of rock samples.

CONCLUSIONS

From regional-scale GDS array studies a crustal anomaly in electrical conductivity has been mapped from southern Wyoming through the Dakotas, Saskatchewan and Manitoba

to Hudson Bay. Tectonic and electrical similarities suggest that there may even be a counterpart of this anomaly in Scandinavia (Jones, 1993). As such, this anomaly, termed the North American Central Plains (NACP) anomaly, is arguably the largest yet discovered on Earth. Camfield and Gough's (1977) suggestion that the NACP is a geophysical marker for a Proterozoic continental collision zone has been shown to be correct, and the NACP can be definitively identified with the Paleoproterozoic Trans-Hudson Orogen.

Magnetotelluric studies over the NACP anomaly from the mid-1980s onwards have shown that the anomaly is not a contiguous or continuous feature, but indeed in section comprises discrete bodies of enhanced conductivity, and is broken along its length.

Lithoprobe studies in 1992 and 1994 have definitively correlated the anomaly at those latitudes with units in the western La Ronge Belt, and the only conductive rocks in that belt belong to the metasedimentary unit Lsn. Within that metasedimentary unit, conductors mapped by airborne EM observations are curvi-linear following, in the main, the structural trend of the region (Standing, 1973). Rock samples from that unit show that the only conductive sequences are sulphides concentrated along the hinges of folds. Accordingly, conclusively identified for this part of the NACP anomaly is the conduction mechanism: electronic conduction in concentrated sulphides in the hinges of folds aligned predominantly along the least compressive stress direction.

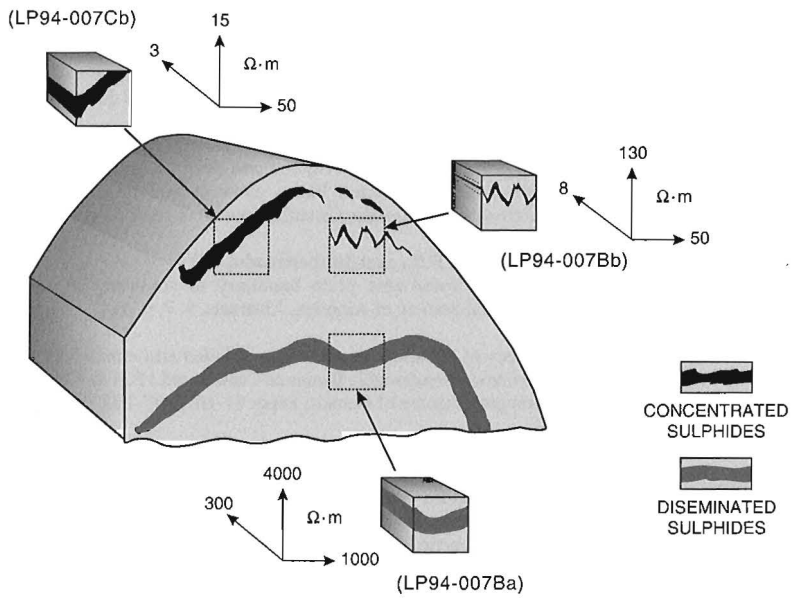

Figure 6.

Schematic representation of a cross-section of sample LP94-007, exemplified by sub-samples LP94-007B and LP94-007C, showing folded layers of sulphide concentrations, and locations from which the second series of sub-samples (LP94-007Cb, LP94-007Bb, LP94-007Ba) were taken. The 3-direction resistivity values of these sub-samples are also displayed.

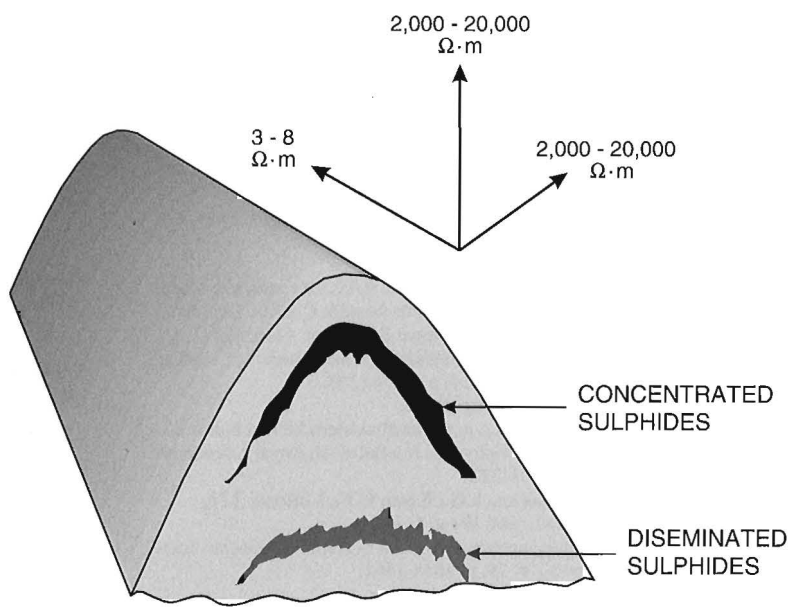

Figure 7.

Electrical model of these rocks, showing folded layers containing highly concentrated sulphides accumulated near the hinge of the fold. This suggests resistivities of 3-8 Ω·m in the direction of the axis, and 2000-20 000 Ω·m in the other two directions, for an anisotropy of 200:1 to 7000:1.

Whether this cause is also operating for the whole length of the anomaly is an open question. The along-strike continuity of the orogen would argue for this being the case. However, the southern terminus of the NACP anomaly, from the Black Hills to southeastern Wyoming (Fig. 1), is likely caused by a different mechanism. Camfield and Gough (1977) noted the spatial correlation of the NACP anomaly at that location with the Hartville Arch, which connects the Black Hills to the Laramie uplift. Within the Hartville Arch are mapped exposures of graphite (Osterwald et al., 1959) and major shear zones and fault systems that continue to the Sierra Madre. Modelling of the GDS responses at the Black Hills shows that the NACP anomaly at that location is both very shallow and highly conductive ($\rho < 1\Omega{\cdot}m$) (Jones and Craven, 1990). Such very low resistivities are necessary to explain that the anomalous horizontal east-west magnetic field is larger than the normal horizontal east-west magnetic field. This part of the conductor also follows the edge of the Wyoming province, rather than within the Trans-Hudson Orogen internides as in the rest of the NACP anomaly. It is possible that the foredeep hypothesis of Boerner et al. (in press) has caused this section of the anomaly. Accordingly, the apparent continuity of the NACP anomaly north and south of the Black Hills could be an artifact of the coarse spatial resolution of the GDS array studies. Rather, there could be two anomalies caused by different conducting mechanisms, one due to sulphides for most of the Trans-Hudson Orogen and one due to graphite at its southern terminus.

ACKNOWLEDGMENTS

The authors are thankful for the critical reviews of this paper by Don White and David Boerner (Geological Survey of Canada).

REFERENCES

API (American Petroleum Institute)
1960: Recommended practices for core-analysis procedure: API Recommended Practice 40 (RP 40) First Edition, American Petroleum Institute, Washington, D.C., p. 55.

Alabi, A.O., Camfield, P.A., and Gough, D.I.
1975: The North American Central Plains anomaly; Royal Astronomical Society Geophysical Journal, v. 43, p. 815-834.

Boerner, D.E., Kurtz, R.D., and Craven, J.A.
in press: Electrical conductivity and Paleoproterozoic foredeeps; Journal of Geophysical Research.

Camfield, P.A. and Gough, D.I.
1975: Anomalies in daily variation magnetic fields and structure under north-western United States and south-western Canada; Geophysical Journal of the Royal Astronomical Society, v. 41, p. 193-218.
1977: A possible Proterozoic plate boundary in North America; Canadian Journal of Earth Sciences, v. 14, p. 1229-1238.

Camfield, P.A., Gough, D.I., and Porath, H.
1970: Magnetometer array studies in the northwestern United States and southwestern Canada; Geophysical Journal of the Royal Astronomical Society, v. 22, p. 201-222.

Clowes, R.M., Cook, F.A., Green, A.G., Keen, C.E., Ludden, J.N., Percival, J.A., Quinlan, G.M., and West, G.F.
1993: Lithoprobe: new perspectives on crustal evolution; Canadian Journal of Earth Sciences, v. 29, p. 1813-1864.

Daly, R.A., Manger, E.G., and Clark, S.P., Jr.
1966: Density of rocks: Section 4; in Handbook of Physical Constants; Geological Society of America, Memoir 97, p. 19-26.

Drury, M.J. and Niblett, E.R.
1980: Buried ocean crust and continental crust geomagnetic induction anomalies: a possible association; Canadian Journal of Earth Sciences, v. 17, p. 961-967.

Dutch, S.I.
1983: Proterozoic structural provinces in the north-central United States; Geology, v. 11, 478-481.

Gough, D.I. and Camfield, P.A.
1972: Convergent geophysical evidence of a metamorphic belt through the Black Hills of South Dakota; Journal of Geophysical Research, v. 77, p. 3168-3170.

Green, A.G., Cumming, G.L., and Cedarwell, D.
1979: Extension of the Superior-Churchill boundary zone into southern Canada; Canadian Journal of Earth Sciences, v. 16, p. 1691-1701.

Green, A.G., Hajnal, Z., and Weber, W.
1985: An evolutionary model of the western Churchill Province and western margin of the Superior Province in Canada and the north-central United States; Tectonophysics, v. 116, p. 281-322.

Gupta, J.C., Kurtz, R.D., Camfield, P.A., and Niblett, E.R.
1985: A geomagnetic induction anomaly from IMS data near Hudson Bay, and its relation to crustal electrical conductivity in central North America; Royal Astronomical Society Geophysical Journal, v. 81, p. 33-46.

Handa, S. and Camfield, P.A.
1984: Crustal electrical conductivity in north-central Saskatchewan: The North American Central Plains anomaly and its relation to a Proterozoic plate margin; Canadian Journal of Earth Sciences, v. 21, p. 533-543.

Hills, F.A., Houston, R.S., and Subbarayudu, G.V.
1975: Possible Proterozoic plate boundary in southern Wyoming; Geological Society of America, Abstracts, v. 7, p. 614.

Hoffman, P.
1981: Autopsy of Athapuscow aulacogen: a failed arm affected by three collisions; in Proterozoic Basins of Canada, (ed.) F.H.A. Campbell; Geological Survey of Canada, Paper 81-10, p. 97-102.

Jones, A.G.
1988: Discussion of A magnetotelluric investigation under the Williston Basin of south-eastern Saskatchewan by J.M. Maidens and K.V. Paulson; Canadian Journal of Earth Sciences, v. 25, p. 1132-1139.
1993: Electromagnetic images of modern and ancient subduction zones; in Plate Tectonic Signatures in the Continental Lithosphere; (ed.) A.G. Green, A. Kroner, H.-J. Gotze and N. Pavlenkova; Tectonophysics, v. 219, p. 29-45.

Jones, A.G. and Craven, J.A.
1990: The North American Central Plains conductivity anomaly and its correlation with gravity, magnetics, seismic and heat flow data in the Province of Saskatchewan; Physics of the Earth and Planetary Interiors, v. 60, p. 169-194.

Jones, A.G. and Savage, P.J.
1986: North American Central Plains conductivity anomaly goes east; Geophysical Research Letters, v. 13, p. 685-688.

Jones, A.G., Craven, J.A., McNeice, G.A., Ferguson, I.J., Boyce, T., Farquarson, C. and Ellis, R.G.
1993: The North American Central Plains conductivity anomaly within the Trans-Hudson orogen in northern Saskatchewan; Geology, v. 21, p. 1027-1030.

Katsube, T.J.
1975: The electrical polarization mechanism model for moist rocks; Report of Activities, Part C; Geological Survey of Canada, Paper 75-1C, p. 353-360.

Katsube, T.J. and Hume, J.P.
1987: Electrical properties of granitic rocks in Lac du Bonnet batholith; in Geotechnical Studies at Whiteshell Research Area (RA-3); CANMET Report MRL 87-52, p. 205-220.

Katsube, T.J. and Mareschal, M.
1993: Petrophysical model of deep electrical conductors; Graphite lining as a source and its disconnection due to uplift; Journal of Geophysical Research, v. 98, B5, p. 8019-8030.

Katsube, T.J. and Salisbury, M.
1991: Petrophysical characteristics of surface core samples from the Sudbury structure; in Current Research, Part E; Geological Survey of Canada, Paper 91-1E, p. 265-271.

Katsube, T.J. and Scromeda, N.
1991: Effective porosity measuring procedure for low porosity rocks; in Current Research, Part E; Geological Survey of Canada, Paper 91-1E, p. 291-297.
1994: Physical properties of Canadian kimberlites; Somerset Island and Saskatchewan; in Current Research 1994-B; Geological Survey of Canada, p. 35-42.
1995: Accuracy of Low Porosity Measurements in Granite; in Current Research 1995-C; Geological Survey of Canada, p. 265-270.

Katsube, T.J. and Walsh, J.B.
1987: Effective aperture for fluid flow in microcracks; International Journal of Rock Mechanics and Mining Sciences and Geomechanics Abstracts, v. 24, p. 175-183.

Katsube, T.J., Best, M.E., and Mudford, B.S.
1991: Petrophysical characteristics of shales from the Scotian shelf; Geophysics, v. 56, p. 1681-1689.

Katsube, T.J., Scromeda, N., and Williamson, M.
1992: Effective porosity of tight shales from the Venture Gas Field, offshore Nova Scotia; in Current Research, Part D; Geological Survey of Canada, Paper 92-1D, p. 111-119.

Katsube, T.J., Scromeda, N., Mareschal, M., and Bailey, R.C.
1992b: Electrical resistivity and porosity of crystalline rock samples from the Kapuskasing Structural Zone; in Current Research, Part E; Geological Survey of Canada, Paper 92-1E, p. 225-236.

Klasner, J.S. and King, E.R.
1986: Precambrian basement geology of North and South Dakota; Canadian Journal of Earth Sciences v. 23, p. 1083-1102.

Keller, G.V.
1982: Electrical properties of rocks and minerals; in Handbook of Physical Properties of Rocks, Vol. I, (ed.) R.S. Carmichael; CRC Press, Inc., Florida, p. 217-293.

Law, L.K. and Riddihough, R.P.
1971: A geographical relation between geomagnetic variation anomalies and tectonics; Canandian Journal of Earth Sciences, v. 8, p. 1094-1106.

Lewry, J.F. and Slimmon, W.L.
1985: Compilation bedrock geology, Lac La Ronge NTS area 73P/73I; Saskatchewan Energy and Mines, Report 225 (1:250 000 scale map with marginal notes)

Lidiak, E.G.
1971: Buried Precambrian rocks of South Dakota; Geological Society of America Bulletin, v. 82, p. 1411-1420.

Maidens, J.M. and Paulson, K.V.
1988: A magnetotelluric investigation under the Williston Basin of southeastern Saskatchewan; Canadian Journal of Earth Sciences, v. 25, p. 60-67.

Nelson, K.D., Baird, D.J., Walters, J.J., Hauck, M., Brown, L.D., Oliver, J.E., Ahern, J.L., Hajnal, Z., Jones, A.G., and Sloss, L.L.
1993: Trans-Hudson orogen and Williston basin in Montana and North Dakota: New COCORP deep profiling results; Geology, v. 21, p. 447-450.

Osterwald, F.W., Osterwald, D.B., Long, J.S., and Wilson, W.H.
1959: Mineral resources of Wyoming; Geological Survey of Wyoming, Bulletin 50, p. 86-87.

Peterman, Z.E.
1981: Dating of Archean basement in northeastern Wyoming and southern Montana; Geological Society of America Bulletin, v. 92, p. 139-146.

Porath, H., Gough, D.I., and Camfield, P.A.
1971: Conductive structures in the northwestern United States and southwest Canada; Geophysical Journal of the Royal Astronomical Society, v. 23, p. 387-398.

Porath, H., Oldenburg, D.W., and Gough, D.I.
1970: Separation of magnetic variation fields and conductive structures in the western United States; Geophysical Journal of the Royal Astronomical Society, v. 19, p. 237-260.

Rankin, D. and Pascal, F.
1990: A gap in the North American Central Plains conductivity anomaly; Physics of the Earth and Planetary Interiors, v. 60, p. 132-137.

Rankin, D. and Reddy, I.K.
1973: Crustal conductivity anomaly under the Black Hills: a magnetotelluric study; Earth and Planetary Science Letters, v. 20, p. 275-279.

Reitzel, J.S., Gough, D.I., Porath, D.I., and Anderson III, C.W.
1970: Geomagnetic deep sounding and upper mantle structure in the western United States; Geophysical Journal of the Royal Astronomical Society, v. 19, p. 213-235.

Scromeda, N. and Katsube, T.J.
1994: Effect of temperature on drying procedures used in porosity measurements of tight rocks; in Current Research 1994-E; Geological Survey of Canada, p. 283-289.

Standing, K.F.
1973: Lac La Ronge conductivity anomaly locations 1:250 000 map; Saskatchewan Energy and Mines, Regina, map 73P.

Thom, A., Arndt, N.T., Chauvel, C., and Stauffer, M.
1990: Flin-Flon and Western La Ronge belts, Saskatchewan: Products of Proterozoic subduction-related volcanism; in The Early Proterozoic Trans-Hudson Orogen of North America, (ed.) J.F. Lewry and M.R. Stauffer; Geological Association of Canada, Special Paper 37, p. 163-176.

Thomas, M.D., Sharpton, V.L., and Grieve, R.A.F.
1987: Gravity patterns and Precambrian structure in the North American Central Plains; Geology, v. 15, p. 489-492.

Geological Survey of Canada Project 870057